



Development of indole/indazole-aminopyrimidines as inhibitors of c-Jun N-terminal kinase (JNK): Optimization for JNK potency and physicochemical properties



Leyi Gong^{a,*}, Xiaochun Han^a, Tania Silva^a, Yun-Chou Tan^a, Bindu Goyal^a, Parch Tivitmahaisoon^a, Alejandra Trejo^a, Wylie Palmer^a, Heather Hogg^a, Alam Jahagir^a, Muzaffar Alam^a, Paul Wagner^a, Karin Stein^a, Lubov Filonova^a, Brad Loe^a, Ferenc Makra^a, David Rotstein^a, Lubica Rapatova^a, James Dunn^a, Fengrong Zuo^b, Joseph Dal Porto^b, Brian Wong^b, Sue Jin^b, Alice Chang^b, Patricia Tran^b, Gary Hsieh^b, Linghao Niu^b, Ada Shao^c, Deborah Reuter^a, Johanness Hermann^a, Andreas Kuglstatter^c, David Goldstein^a

^a Department of Medicinal Chemistry, Roche Palo Alto, Palo Alto, CA 94304, USA

^b Inflammation Therapeutic Area, Roche Palo Alto, Palo Alto, CA 94304, USA

^c Department of Discovery Technologies, Roche Palo Alto, Palo Alto, CA 94304, USA

ARTICLE INFO

Article history:

Received 19 February 2013

Revised 8 April 2013

Accepted 12 April 2013

Available online 21 April 2013

Keywords:

JNK

JNK inhibitors

Aminopyrimidine

c-Jun N-terminus kinase

Kinase inhibitors

ABSTRACT

A novel series of indole/indazole-aminopyrimidines was designed and synthesized with an aim to achieve optimal potency and selectivity for the c-Jun kinase family or JNKs. Structure guided design was used to optimize the series resulting in a significant potency improvement. The best compound (**17**) has IC₅₀ of 3 nM for JNK1 and 20 nM for JNK2, with greater than 40-fold selectivity against other kinases with good physicochemical and pharmacokinetic properties.

© 2013 Elsevier Ltd. All rights reserved.

The c-Jun N-terminal kinases (JNKs) are a family of serine/threonine protein kinases of the mitogen-activated protein kinase (MAPK) group along with p38 and ERK.^{1–3} JNKs can be expressed as 10 different isoforms by mRNA alternative splicing of three highly related genes, JNK1, JNK2 and JNK3.⁴ While JNK1 and JNK2 are found to be ubiquitously expressed, JNK3 is principally present in the brain, cardiac muscle, and testis.⁵ Based on the role of JNK in regulating members of the activator protein-1 (AP-1) transcription factors and other cellular factors implicated in gene expression, cellular survival and proliferation in response to cytokines and growth factors, inhibiting JNK may have many potential therapeutic utilities.^{6,7} Consequently, many chemotypes of JNK inhibitors have been reported in the literature.^{8–19}

JNK plays a critical role in T cell signaling and has been shown to regulate the expression or function of a number of proinflammatory cytokines (TNF α , IL-2, IL-6, etc.), that are central to many human inflammatory disorders.⁶ As such, JNK inhibitors have the potential to be immuno-modulatory agents and are of therapeutic

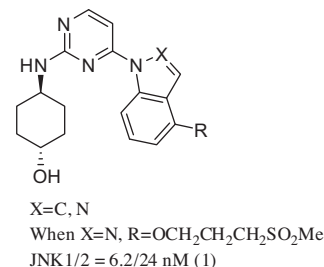


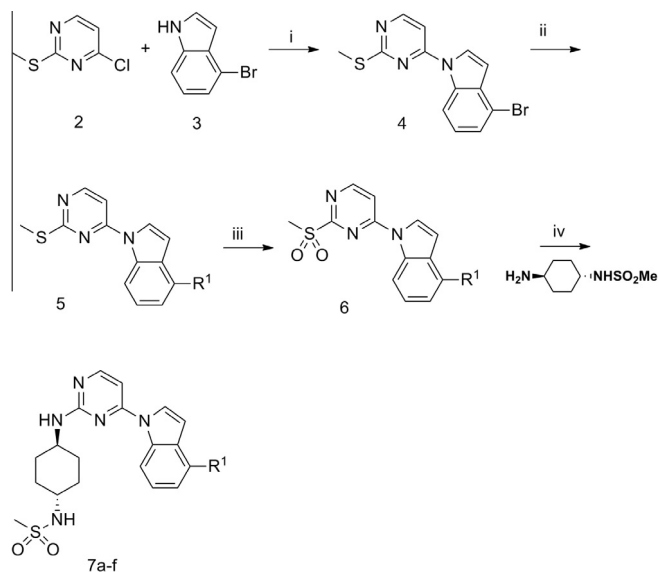
Figure 1. Aminopyrimidine JNK inhibitors.

interest for the treatment of rheumatoid arthritis and asthma. Since both JNK1 and JNK2 are implicated, dual JNK1/2 inhibitors were developed.

In our previous letter, we described our effort on optimizing kinase selectivity with different heterocycles attached to the aminopyrimidine core shown in Figure 1 and demonstrated that indole and indazole scaffolds afforded the favorable selectivity and physicochemical properties we desired.²⁰ Here, we wish to report our

* Corresponding author. Tel.: +1 650 859 4306; fax: +1 650 859 3153.

E-mail address: leyi.gong@sri.com (L. Gong).

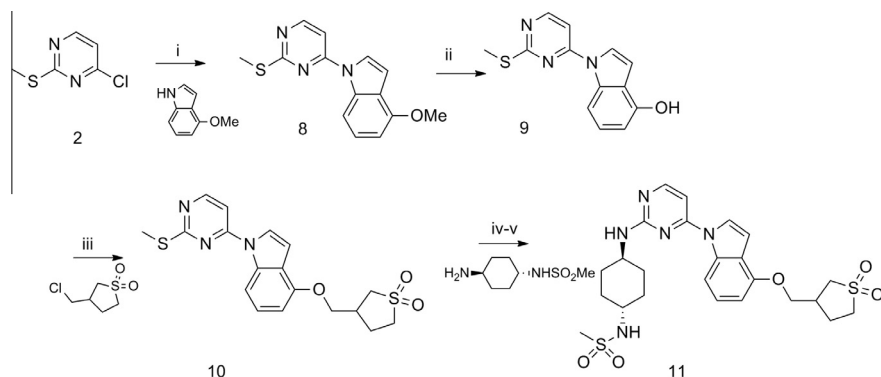


Scheme 1. Reagents and conditions: (i) NaH in DMF (0–25 °C), 50–60%; (ii) amine (R_1NH), NaOtBu, bis(tri-*t*-Bu-phosphine)Pd (0) in dioxane, 40–50%; (iii) 4-Cl-PhCO₃H in CH₂Cl₂, 0 °C, 2 h, 95–100% without purification; (iv) 4–5 equiv of NEt₂(*i*Pr), 100 °C in NMP, 60–70%.

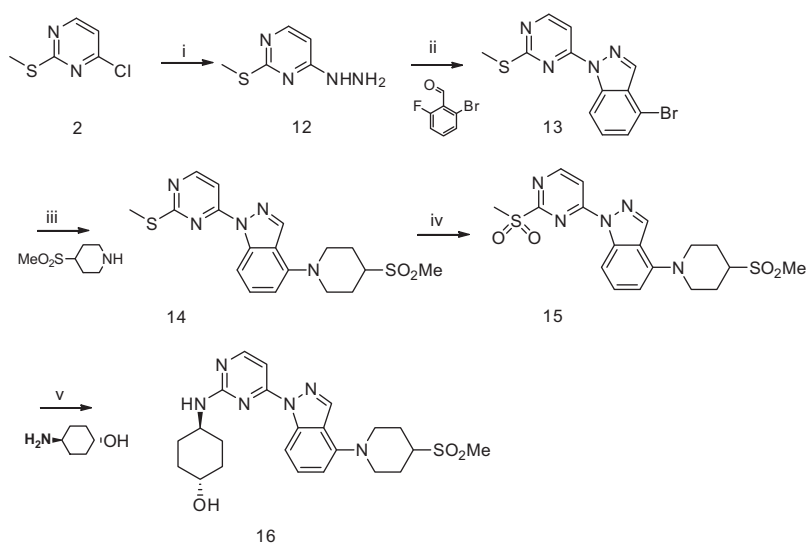
continued effort on further optimizing the potency and properties of this series.

Most of compounds in this study were synthesized by appropriate substitution of 4-chloro-2-thiomethyl-diaminopyrimidine according to the Schemes 1–4.

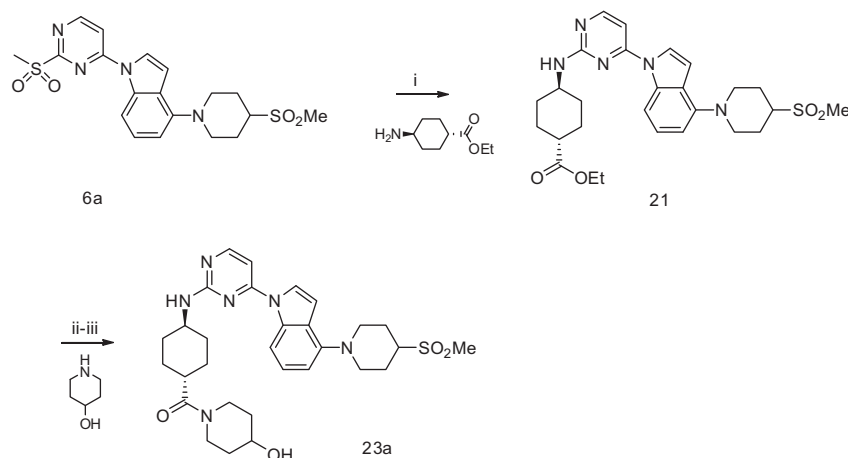
Analogs (**7a–f**) were synthesized according to Scheme 1. Displacement of 4-Cl-2-thiomethyl-pyrimidine (**2**) with 4-bromoindole and sodium hydride in DMF afforded the intermediate (**4**). Amination of **4** with secondary amines such as piperazine and piperidine using traditional conditions such as Pd(PPh₃)₄ and NaOMe, yielded mostly the des-bromo indole by-product and gave low yields of the desired products (**5a–f**). This is presumably due to a slow reductive elimination step in the Pd-catalytic cycle presented by the steric bulkiness of the secondary amine (e.g., piperidine methyl-sulfone). To facilitate the rate of the elimination step, steric hindered phosphine ligand (*t*-Bu₃P) was used.²¹ Using the pre-formed bis(tri-*t*-butylphosphine)-palladium(0) in combination with sodium *t*-butoxide was the most effective condition for this transformation and improved the yields. The methyl-sulfide **5a–f** was then oxidized using 3-chloro-perbenzoic acid (*m*-CPBA) and the resulting sulfoxide or sulfone was displaced with 1-methyl sulfonylamino-4-aminocyclohexane without further isolation to give the final products (**7a–f**).



Scheme 2. Reagents and conditions: (i) NaH in DMF, 0–25 °C, 55%; (ii) BBr₃ in CH₂Cl₂, 0–25 °C, 2 h, 85–95%; (iii) K₂CO₃, 100 °C in NMP, 45–55%; (iv) 4-Cl-PhCO₃H in CH₂Cl₂, 0 °C, 2 h, 95–100% without purification; (v) 4–5 equiv of NEt₂(*i*Pr), 100 °C in NMP, 60–70%.



Scheme 3. Reagents and conditions: (i) 4–5 equiv of NEt₂(*i*Pr), 100 °C in NMP, 60–70%; (ii) 5 equiv NaOH in EtOH, 80 °C, 95%; (iii) NaOtBu, bis(tri-*t*-Bu-phosphine)Pd (0) in dioxane, 50%; (iv) 4-Cl-PhCO₃H in CH₂Cl₂, 0 °C, 2 h, 95–100% without purification; (v) 4–5 equiv of NEt₂(*i*Pr), 100 °C in NMP, 60–70%.



Scheme 4. Reagents and conditions: (i) 4–5 equiv of $\text{NEt}_2(\text{iPr})$, 100 °C in NMP, 60–70%; (ii) 5 equiv NaOH in EtOH, 80 °C, 95%; (iii) EDCI in CH_2Cl_2 , rt, overnight, 80–85%.

Table 1
Cyclic side chains

	R_1	JNK1/JNK2 IC_{50} (nM) ^a	c-Jun IC_{50} (μM) ^a
1		6.2/24	1.0
7a		3/24	0.71
7b		29/180	na
7c		5/36	0.20
7d		10/68	0.82
7e		94/650	na
7f		44/280	na
11		6.8/35	0.104

Cellular activity was measured based on the description in Ref. 24; na = no data obtained.

^a Compounds were characterized by mass spectral, ^1H NMR, elemental analysis and mp. IC_{50} values are an average of multiple determinations ($n \geq 2$). Assay conditions are described in Ref. 23.

Similarly, 4-methoxyindole with NaH in DMF readily gave the intermediate (**8**), which was reacted with boron tribromide to give the de-methylated phenol derivative (**9**). Alkylation of **9** with chloromethyl tetrahydro-thiophene dioxide at 100 °C in dioxane in the presence of potassium carbonate yielded compound **10**, which was converted to the final product (**11**) by oxidation and

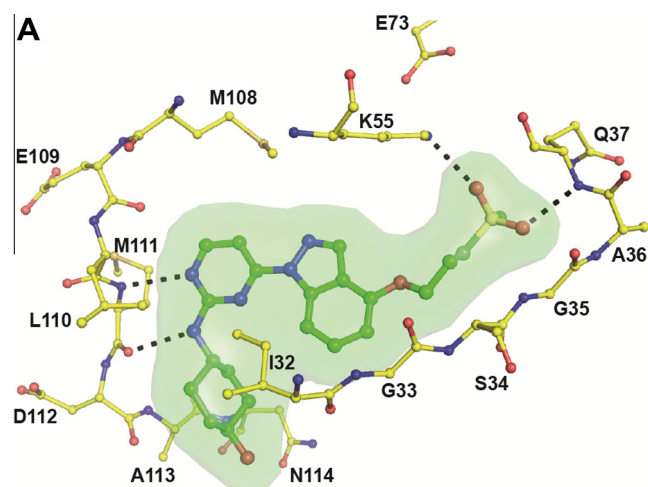


Figure 2. X-ray structure of compound **1** bound to JNK1 β .^{20,22}

the subsequent replacement with (*trans*)-*N*-methylsulfonyl diaminocyclohexane described in Scheme 2.

The indazole analogs were synthesized via a slightly different route shown in Scheme 3. Regioisomers were obtained if indazole was reacted with **2** directly under a basic condition such as NaH. Therefore, 4-chloro-2-thiomethyl pyrimidine was mixed with hydrazine to give **12**, which upon reacting with 2-bromo-6-fluorobenzaldehyde was converted to **13** in a region-specific and high yielding fashion. Similar palladium mediated aromatic amination shown in Scheme 1, procedure (ii) was used for the transformation of **13** and **14**. Subsequent oxidation afforded **15** and nucleophilic replacement with 4-hydroxy-cyclohexyl amine provided **16**.

Analog with modification at the distal end of cyclohexyl ring in Table 2 were synthesized according to Scheme 4.

Nucleophilic substitution of **6a** by various cyclohexyl derived amines gave compounds **17–22c**. For example, the use of *trans*-4-hydroxy-cyclohexylamine afforded **17** whereas the use of 4-acetyl-amino-cyclohexylamine and 4-OH-4-Me-cyclohexylamine provided **18** and **19**, respectively. On the other hand, *trans*-4-ethylcarboxyl-cyclohexylamine gave **20** and **21**. Compound **21** then underwent saponification and EDCI mediated amide coupling to produce compound **22a–c** as described in Scheme 4.

X-ray crystal structure of compound **1** bound to the JNK1 β shown in Figure 2 provided the basis for the design of analogs with improved potency and physicochemical properties.

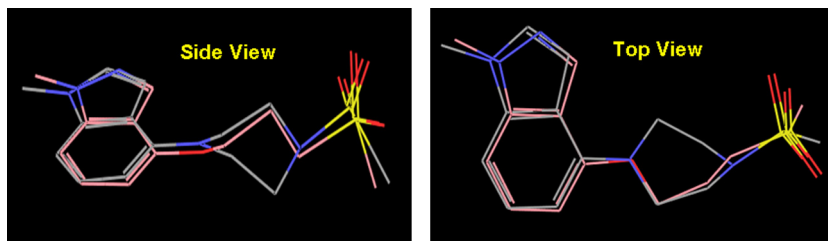
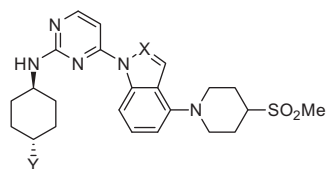


Figure 3. Overlay of the linear side chain in **1** (in pink color) with the cyclic side chain in **7b** in gray color.

Table 2
Activities of compounds with varying front groups



Compds	X	Y	JNK1/2 IC ₅₀ (nM) ^a	c-Jun IC ₅₀ (μM) ^a
7a	C	NHSO ₂ Me	3/24	0.7
16	N	OH	6/17	0.29
17	C	OH	3/20	0.24
18	C	NHCOMe	7/49	0.7
19	C	Me(OH)	12/66	1.3
20	N	CO ₂ Et	na/27	1.7
21	C	CO ₂ Et	7/40	1.3
22a	C		8/33	0.65
22b	C		12/86	0.42
22c	C		na/12	0.22

^a Values are means of three experiments (na = not measured).

As **Figure 2** indicated, the indazole-aminopyrimidine of **1** interacted with the backbone amino acids (Met111, Leu110 and Glu109) via two hydrogen bonds (as highlighted by the dashed

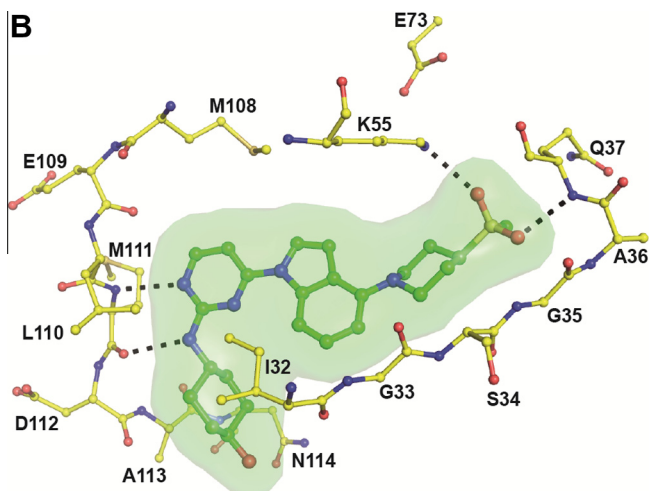


Figure 4. X-ray structure of compound **17** bound to JNK1β.²⁵

Table 3
Physicochemical properties

Compds	PSA	Solubility ^a	CACO ₂ (AB) ^b	ER ^c
16	98	3.5	3.8	5
17	84	5.2	10.5	2
22a	101	43	0.4	53
22c	113	21	0.1	94

^a Solubility was measured in a standard PO₄ buffer system with pH of 6.4, unit: μg/mL.

^b Unit: ×10⁻⁶ cm/min.

^c ER = AB/BA.

Table 4
Pharmacokinetic data of **17**

Species	Route	Cl ^a	T _{1/2} ^b	% F ^c
Rat	IV ^d	47	0.7	–
	PO ^e	–	2	100
Dog	IV ^d	10.6	4.5	–
	PO ^e	–	3.4	15

^a Unit: ml/min-kg.

^b Unit: h.

^c Oral bioavailability.

^d Dose: 0.5 mpk.

^e Dose: 2 mpk.

lines in black color) in a classical donor-acceptor pair hinge interaction. A closer examination of the bound conformation of **1** revealed that the side chain was tucked under the glycine-rich-loop via hydrophobic interaction. Furthermore, the side chain (OCH₂CH₂CH₂SO₂Me) adopted the gauche conformation. It was rationalized that cyclic ring systems, particularly six member ring systems in chair conformation could mimic the linear gauche conformation. In addition, cyclic side chains would provide different kinase selectivity profile and different physicochemical properties than the linear ones. As such, a number of cyclic ring systems were evaluated using ROCS, the modeling tool from OpenEye Scientific Software. Shown in **Figure 3** is the overlay view of a linear side chain with a cyclic one using ROCS.

Table 5
Kinase selectivity profile of **17**^c

Kinase	Fold ^a	Kinase	Fold ^a	Kinase	Fold ^a
JNK1	1 ^b	p38-δ	150	SgK085	700
JNK2	6	IRAK1	193	MAPK7	786
IKK-β	46	DAPK3	264	DCAMKL3	786
p38-γ	71	MAPK15	364	RIOK2	857
STK17A	71	DAPK2	371	CDK7	929
DAPK1	107	MAP2K4	393	RPS6KA1	1786

^a Fold = Kd of a kinase/Kd of JNK1.

^b Kd of JNK1 = 0.14 nM.

^c The rest of kinases in the commercial kinase panel (unlisted in this table) have fold over JNK1 of >2000; all Kds were determined in ambit.

Compounds (**7a–f**, **11**) in Table 1 were synthesized based on the near perfect shape match in Figure 3.

Compounds **7a** containing the 4-SO₂Me-piperidine and **11** incorporating an oxymethyl tetrahydrothiophene dioxide cyclic side chains are equipotent with **1** containing a liner side chain.

Furthermore, it was evident that a H-bond acceptor at the end of a side chain was important for the potency as one compares compound **7a** with **7e**. The difference in potency between compound **7a** and **7b** or **7a** and **7f** can be explained on the basis of the orientation of the acceptor. In addition, acetyl piperazine side chains in **7c** and **7d** were slightly less potent than sulfonyl piperidine (**7a**).

To further explore the SAR around this series, modification of the group at the distal end of cyclohexyl amine, labeled as Y were pursued (Table 2). In general, a diverse set of Y groups were well tolerated (**16–22c**). With Figures 2 and 4, one could rationalize this based on the fact that Y groups were situated in a more solvent exposed region. The impact of a Y group was more reflected on polarity and molecular weight of a compound, thus the physicochemical properties, and less on the potency. Moreover, indole and indazole analogs were equipotent (**16** vs **17** and **20** vs **21**).

Figure 4 confirms that the bound conformation of cyclic piperidine side chain in **17** in X-ray structure of JNK1 β protein perfectly mimics the conformation of the linear side chain in **1** (Fig. 2).

Table 3 exhibits some of the physicochemical properties of representative compounds including solubility, permeability and the efflux ratio (ER).

It is apparent that the intrinsic permeability of these compounds decreased when their PSA exceeded 100 (Table 3). It appears that as this series of compounds got more polar, it was more likely to be a substrate of PGP transporters based on the high efflux ratio. Compound **17** displayed overall balanced profile and was chosen for further evaluation. Table 4 highlights some of the PK parameters obtained for **17** in both rats and dogs. The rat clearance rate for **17** was high, but dog clearance rate was medium. The oral bioavailability in both species was good enough to enable further in-vivo characterization of **17** in these species.

Kinase selectivity of **17** was then profiled against 317 kinases in a commercial kinase panel.^{26,27} **17** exhibited 40-fold selectivity for the JNK subfamily over other kinases shown in Table 5.

Based on its good pharmacokinetic property demonstrated in rat and in dogs as well as its excellent kinase selectivity profile, compound (**17**) serves as a superb tool molecule for studying JNK pharmacology. The efficacy of **17** in various disease models will be presented in due course.

In summary, a series of potent and selective indole-aminopyrimidine inhibitors was discovered and developed using structure based drug design. Compound **17**, a potent and selective JNK inhibitor from the series, exhibited excellent physicochemical and pharmacokinetic properties.

References and notes

- Derijard, B.; Hibi, M.; Wu, I. H.; Barrett, T.; Su, B.; Deng, T.; Karin, M.; Davis, R. J. *Cell* **1994**, *76*, 1025.
- Kallunki, T.; Su, B.; Tsigelny, I.; Sluss, H. K.; Derijard, B.; Moore, G.; Davis, R.; Karin, M. *Genes Dev.* **1994**, *8*, 2996.
- Kyriakis, J. M.; Avruch, J. *J. Biol. Chem.* **1990**, *265*, 17355.
- Grupta, S.; Barrett, T.; Whitmarsh, A. J.; Cavanagh, J.; Sluss, H. K.; Derijard, B.; Davis, R. J. *EMBO J.* **1996**, *15*, 2760.
- Martin, J. H.; Mohit, A. A.; Miller, C. A. *Mol. Brain Res.* **1996**, *35*, 47.
- Manning, A. M.; Davis, R. J. *Nat. Rev. Drug Disc.* **2003**, *2*, 554.
- Wellen, K. E.; Hotamisligil, G. S. *J. Clin. Invest.* **2005**, *115*, 1111.
- Asano, Y.; Kitamura, S.; Ohra, T.; Aso, K.; Igata, H.; Tamura, T.; Kawamoto, T.; Tanaka, T.; Sogabe, S.; Matsumoto, S.; Yamaguchi, M.; Kimura, H.; Itoh, F. *Bioorg. Med. Chem.* **2008**, *16*, 4699.
- Asano, Y.; Kitamura, S.; Ohra, T.; Itoh, F.; Kajino, M.; Tamura, T.; Kaneko, M.; Ikeda, S.; Igata, H.; Kawamoto, T.; Sogabe, S.; Matsumoto, S.; Tanaka, T.; Yamaguchi, M.; Kimura, H.; Fukumoto, S. *Bioorg. Med. Chem.* **2008**, *16*, 4715.
- Liu, G.; Zhao, H.; Liu, B. *Bioorg. Med. Chem. Lett.* **2007**, *17*, 495.
- Szczepankiewicz, B. G.; Kosogof, C.; Nelson, L. T.; Liu, G.; Liu, B.; Zhao, H.; Serby, M. D.; Xin, Z.; Liu, M.; Gum, R. J.; Haasch, D. L.; Wang, S.; Clampit, J. E.; Johnson, E. F.; Lubben, T. H.; Stashko, M. A.; Olejniczak, E. T.; Sun, C.; Dorwin, S. A.; Haskins, K.; Abad-Zapatero, C.; Fry, E. H.; Hutchins, C. W.; Sham, H. L.; Rondinone, C. M.; Trevillyan, J. M. *J. Med. Chem.* **2006**, *49*, 3563.
- Zhao, H.; Serby, M. D.; Xin, Z.; Szczepankiewicz, B. G.; Liu, M.; Kosogof, C.; Liu, B.; Nelson, L. T.; Johnson, E. F.; Wang, S.; Pederson, T.; Gum, R. J.; Clampit, J. E.; Haasch, D. L.; Abad-Zapatero, C.; Fry, E. H.; Rondinone, C.; Trevillyan, J. M.; Sham, H. J.; Liu, G. *J. Med. Chem.* **2006**, *49*, 4455.
- Liu, G.; Zhao, H.; Liu, B.; Xin, Z.; Liu, M.; Serby, M. D.; Lubbers, N. L.; Widomski, D. L.; Polakowski, J. S.; Beno, D. W. A.; Trevillyan, J. M.; Sham, H. L. *Bioorg. Med. Chem. Lett.* **2006**, *16*, 5723.
- Christopher, J. A.; Atkinson, F. L.; Bax, B. D.; Brown, M. J.; Champigny, A. C.; Chuang, T. T.; Jones, E. J.; Mosley, J. E.; Musgrave, J. R. *Bioorg. Med. Chem. Lett.* **2009**, *19*, 2230.
- Alam, M.; Beevers, R. E.; Ceska, T.; Davenport, R. J.; Dickson, K. M.; Fortunato, M.; Gowers, L.; Haughan, A. F.; James, L. A.; Jones, M. W.; Kinsella, N.; Lowe, C.; Meissner, J. W. G.; Nicolas, A.; Perry, B. G.; Phillips, D. J.; Pitt, W. R.; Platt, A.; Ratcliffe, A. J.; Sharpe, A.; Tait, L. J. *Bioorg. Med. Chem. Lett.* **2007**, *17*, 3463.
- Stocks, M. J.; Barber, S.; Ford, R.; Leroux, F.; St-Gallay, S.; Teague, S.; Xue, Y. *Bioorg. Med. Chem. Lett.* **2005**, *15*, 3459.
- De, S. K.; Chen, V.; Stebbins, J. L.; Chen, L.; Cellitti, J. F.; Machleidt, T.; Barile, E.; Riel-Mehan, M.; Dahl, R.; Yang, L.; Emdadi, A.; Murphy, R. *Bioorg. Med. Chem.* **2010**, *18*, 590.
- Kamenecka, T.; Jiang, R.; Song, X.; Duckett, D.; Chen, W.; Ling, Y. Y.; Habel, J.; Laughlin, J. D.; Chambers, J.; Figueroa-Losada, M.; Cameron, M. D.; Lin, L.; Ruiz, C. H.; LoGrasso, P. V. *J. Med. Chem.* **2010**, *53*, 419.
- Noël, R.; Shin, Y.; Song, X.; Koenig, M.; Chen, W.; Ling, Y. Y.; Lin, L.; Ruiz, C. H.; LoGrasso, P.; Cameron, M. D.; Duckett, D. R.; Kamenecka, T. M. *Bioorg. Med. Chem. Lett.* **2011**, *21*, 2732.
- Palmer, W. S.; Alam, M.; Arzeno, H. B.; Chang, K. C.; Dunn, J. P.; Goldstein, D. M.; Gong, L.; Goyal, B.; Hermann, J. C.; Hogg, J. H.; Hsieh, G.; Jahangir, A.; Janson, C.; Jin, S.; Ursula, K. R.; Kuglstatler, A.; Lukacs, C.; Michoud, C.; Niu, L.; Reuter, D. C.; Shao, A.; Silva, T.; Trejo-Martin, T. A.; Stein, K.; Tan, Y.; Tivitmahaisoon, P.; Tran, P.; Wagner, P.; Weller, P.; Wu, S. *Bioorg. Med. Chem. Lett.* **2013**, *23*(5), 1486.
- Tolman, C. A. *Chem. Rev.* **1977**, *77*, 313–348.
- PDB accession number: 4HYU, 2.15 Å resolution.
- JNK activity was measured by phosphorylation of GST-ATF2 (19–96) with [γ -³³P] ATP. The enzyme reaction was conducted at Km concentrations of ATP and the substrate final volume of 40 μ l in buffer containing 25 mM HEPES, pH 7.5, 2 mM dithiothreitol, 150 mM NaCl, 20 mM MgCl₂, 0.001% Tween[®] 20, 0.1% BSA and 10% DMSO. Human JNK2 α 2 assay contains 1 nM enzyme, 1 μ M ATF2, 8 μ M ATP with 1 μ Ci [γ -³³P] ATP. Human JNK1 α 1 assay contains 2 nM enzyme, 1 μ M ATF2, 6 μ M ATP with 1 μ Ci [γ -³³P] ATP. The enzyme assay was carried out in the presence or absence of several compound concentrations. JNK and compound were pre-incubated for 10 min, followed by initiation of the enzymatic reaction by adding ATP and the substrate. The reaction mixture was incubated at 30 °C for 30 min. At the end of incubation, the reaction was terminated by transferring 25 μ l of the reaction mixture to 150 μ l of 10% glutathione Sepharose[®] slurry (Amersham #27-4574-01) containing 135 mM EDTA. The reaction product was captured on the affinity resin, and washed on a filtration plate (Millipore, MABVNOB50) with phosphate buffered saline for six times to remove free radionucleotide. The incorporation of ³³P into ATF2 was quantified on a microplate scintillation counter (Packard Topcount). Compound inhibition potency on JNK was measured by IC₅₀ value generated from 10 concentration inhibition curves fitted into the 3-parameter model: % inhibition = maximum/(1 + (IC₅₀/[inhibitor])^{3lope}). Data were analyzed on Microsoft Excel for parameter estimation. For details, please see: Gong, L. WO Patent 138,340, 2009.
- c-Jun activation assay in TNF α -induced human chondrosarcoma SW1353 cells: SW1353 cells are grown in DMEM (invitrogen) with 10% fetal bovine serum (invitrogen). Ascorbic acid (15 mg/ml), penicillin (100 U/ml) and streptomycin (100 mg/ml) (invitrogen). Cells are plated at a density of 8000 cell per well in 100 ml of growth media for 24 h before the compound treatment. Immediately before the treatment, media is replaced with 90 ml of fresh media, then add 10 ml of 10 \times concentrated compound solution and allowed to pre-incubate with cells for 30 min. The vehicle (DMSO) is maintained at a final concentration of 0.5% in all samples. After 30 min, the cells are activated with 10 ng/ml of TNF α (Roche Biochemical) and incubated 20 min at 37 °C in 5% CO₂. Cells are fixed in 4% formaldehyde/PBS and permeabilized with 0.5% Triton-100/PBS (Roche Biochemical), then were incubated in blocking buffer (2% BSA/PBS) for 1 h. The cell are stained with c-Jun monoclonal antibody (Santa Cruz Biotechnology) for 1 h and detected with DyLight 488 Goat anti-mouse antibody (Thermo Fisher), nuclei are stained with Hoechst dye (Thermo Fisher). Images are acquired and quantified by ArrayScan reader (Thermo Fisher). The IC₅₀ values are calculated as the concentration of the compound at which the c-Jun intensity was reduced to 50% of the control value using Xlfit in Microsoft Excel program.
- PDB accession number: 4IZY, 2.3 Å resolution.
- Bamborough, P.; Drewry, D.; Harper, G.; Smith, G. K.; Schneider, K. J. *Med. Chem.* **2008**, *51*, 7898.
- Goldstein, D. M.; Gray, N. S.; Zarrinkar, P. P. *Nat. Rev. Drug Disc.* **2008**, *7*, 391.